Volume 12, No 1 | International Journal of Radiation Research, January 2014

Three-dimensional gel dosimetry for dose volume histogram verification in compensator-based IMRT

M. Keshtkar[1,2*], A. Takavar[1], M.H. Zahmatkesh[3], H.A. Nedaie[1], A. Vaezzadeh[1], M. Naderi[4]

[1]*Department of Medical Physics and Biomedical Engineering, Tehran University of Medical Sciences, Tehran, Iran*
[2]*Department of Medical Physics, Isfahan University of Medical Sciences, Isfahan, Iran*
[3]*Novin Institute of Medical Radiation, Shahid Beheshti University of Medical Sciences, Tehran, Iran*
[4]*Department of Radiotherapy - Oncology, Tehran University of Medical Sciences, Tehran, Iran*

► ***Original article***

**** Corresponding author:***
Mr. Mohammad Keshtkar,
Fax: *+98 21 88973653*
E-mail:
Keshtkar.dmohammad@yahoo.com

Submitted: July 2013
Accepted: Oct. 2013

Int. J. Radiat. Res., January 2014; 12(1): 13-20

ABSTRACT

Background: Some tissues in human body are radiobiologically different from water and these inhomogeneity must be considered in dose calculation in order to achieve an accurate dose delivery. Dose verification in complex radiation therapy techniques, such as intensity-modulated radiation therapy (IMRT) calls for volumetric, tissue equivalent and energy independent dosimeter. The purpose of this study is to verify a compensator-based IMRT plan in anthropomorphic inhomogeneous phantom by Dose Volume Histograms (DVH) using polymer gel dosimetry. ***Materials and Methods***: An anthropomorphic pelvic phantom was constructed with places for gel inserts. Two attached cubic inserts for prostate and bladder and a cylindrical insert for rectum. A prostate treatment case was simulated in the phantom and the treatment was delivered by a five field compensator-based IMRT. Gel dosimeters were scanned by a 1.5 Tesla magnetic resonance imaging (MRI). Results were analyzed by DVH and difference of differential DVH. ***Results***: Results showed for 3D compensator-based IMRT treatment plan for prostate cancer, there was overall good agreement between calculated dose distributions and the corresponding gel measured especially in planning target volume (PTV) region. ***Conclusion***: Our measurements showed that the used treatment plan configuration has had clinically acceptable accuracy and gel dosimetry can be considered as a useful tool for measuring DVH. It may also be used for quality assurance and compensator-based IMRT treatment verification.

Keywords: *Heterogeneity, polymer gel dosimetry, compensator-based IMRT, dose verification.*

INTRODUCTION

Some tissues in human body are radiobiologically different from water and these inhomogeneities must be considered in dose calculation in order to achieve an accurate dose delivery. In other words, to maximize therapeutic benefit of radiation therapy, absorbed dose that would be delivered in the presence of inhomogeneity must be predicted accurately [1]. Investigation of coincidence of predicted 3D dose distribution by treatment planning calculation with corresponding to actual delivered is one the most important stages in radiation therapy [2, 3]. Treatment verification can be fulfilled by many dosimetry tools. Dosimeters like ionization chambers, TLD, diode and film are dimensionally limited. Gel have more dose sensitivity (slope of the calibration curve) and higher dose sensitivity

[Downloaded from ijrr.com on 2026-11-08]

dosimetry is capable to capture dose distribution in three dimensions. Furthermore, gel dosimeters are tissue equivalent and have no significant energy dependence [4, 5]. The history of development of gel dosimetry has been mentioned in many papers [4], but the most notable development was in 2001, when Fong *et al.* introduced a new polymer gel dosimeter that was fabricated in the presence of oxygen known as MAGIC (Methacrylic and Ascorbic acid in Gelatin Initiated by Copper) [6]. This development in gel dosimetry paved the way for fabricating gels on the bench top in laboratory.

There are many techniques for delivering radiotherapy treatment and intensity modulated radiation therapy (IMRT) is one of them. Although MLC-based IMRT techniques are the widely accepted techniques nowadays, compensator-based IMRT is an alternative way to deliver the intensity modulated treatment. Compensator-based IMRT has advantages over MLC-based IMRT such as simplicity, making continuously varying intensity modulation, shorter treatment time, simple and rapid quality assurance, but the main disadvantage of this technique is lack of automation [7-14]. Compensators produce an optimized primary fluence profile at the patient's surface and perturbs beam by hardening the primary photon spectrum and generating scattered photons and electrons [15, 16]. From the attenuation equations with the consideration of beam divergence and beam hardening, the compensator thickness can be calculated and then construction can be done by milling machine [10].

Dose verification by gel dosimetry and its application in IMRT and tomotherapy have been investigated by many researchers [17-25, 3]. To the author's knowledge, despite of many studies for MLC-based IMRT, there are a few publications about application of gel dosimetry in compensator-based IMRT [26, 27] and it should be noted that inhomogeneous phantom has not been used in these publications. In this paper, the goal is to verify three dimensionally a compensator-based IMRT plan in cause more dose resolution [5]; MAGIC gel and MRI were employed in this work.

MATERIALS AND METHODS

Phantom design

An anthropomorphic inhomogeneous pelvic phantom based on CT slices that obtained from a patient study was designed and fabricated (figure 1). The phantom consists of slices which are integrated to form a human pelvis. Individual slices were machined with corresponding body contour, related organs (prostate, bladder and rectum) and pelvic bone (figure 2). Two attached cubic inserts with dimensions of 3.5×3.5×4 cm^3 and 6×6×7 cm^3 for prostate and bladder respectively and cylindrical one with diameter of 3 cm and 7 cm height for rectum (herein we call them organ-specific inserts) determined for gel dosimetry. It should be noted that dimensions of organ-specific inserts were manufactured in such a way that they would fit in the pelvic phantom. The phantom and gel inserts were made of Poly methyl-methacrylate (PMMA), while the pelvic bone and femurs were made of bone equivalent material, polytetrafluoroethylene (PTFE).

Gel manufacturing

The composition of MAGIC gel and procedure for its manufacturing was the same as mentioned in Fong *et al.* [6]. Due to the toxicity of some materials; gel preparation was carried out in a fume cupboard. After preparation, the MAGIC gel was poured into organ-specific inserts and calibration vials. In order to perform dose response calibration, a set of gel filled screw-top glass vials (inner diameter 14 mm, length 10 cm) was employed. All gels were allowed to set in a refrigerator.

Compensator-based IMRT treatment case and irradiation

For treatment planning, organ-specific inserts were filled with water and then inserted anthropomorphic phantom by polymer gel dosimetry. Since the MAGIC gel-MRI method into pelvic phantom. Because the gel is nearly water equivalent [6], it can be assumed that it has no significant effect on the absorbed dose

[Downloaded from ijrr.com on 2026-11-08]

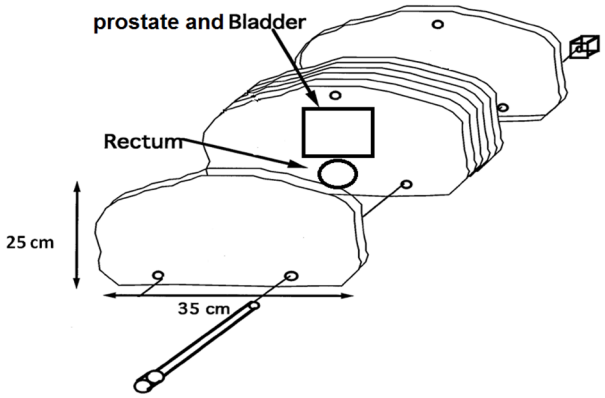


Figure 1. Components of the fabricated phantom, note that cubic insert for prostate is positioned and attached to bladder one in such away they make one integrated volume.

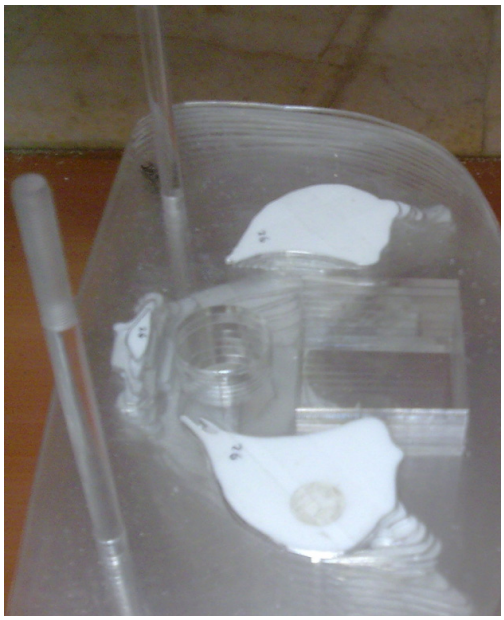
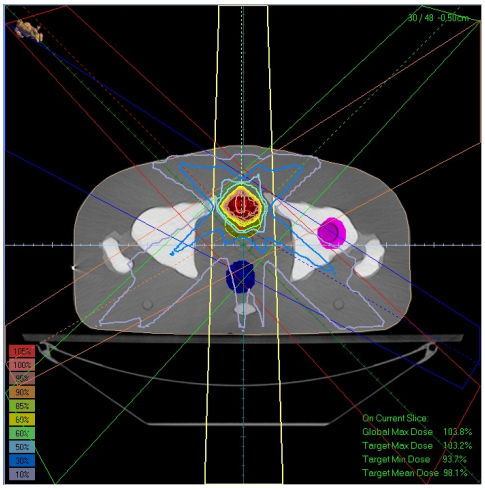


Figure 2. The opened slice anthropomorphic phantom.

calculations. Pelvic phantom was imaged by a computerized tomography (CT) scanner. Three fiducial markers were stuck on the phantom to simplify positioning during CT scanning and IMRT delivery. The thickness of CT slices was 5 mm and 48 images were acquired without any gap between slices.

For this work, TiGRT treatment planning system was employed. After importing the CT images into the treatment planning software (TPS), structures were delineated; rectum in cylindrical insert, bladder and prostate in cubic inserts. Fractional doses were 8 Gy and treatment with 18 MV photons was selected. Then a compensator-based intensity modulated treatment plan (intensity-map based optimization) with five coplanar beams was generated by TPS (figure 3). Data related to compensators were exported; these data for each compensator consist of a spread sheet that the number value into each point shows the height of compensator in that point. For manufacturing compensator molds, these values were imported into AutoCAD software point by point and the map of each compensator was planned in a 10×10 cm plane. According to these maps, laser cutting machine (CO_2) cut slices of molds with material of Perspex; Perspex slices of each compensator were attached together tightly, and then were filled by melted cerrobend. After enough cooling, compensators were extracted.



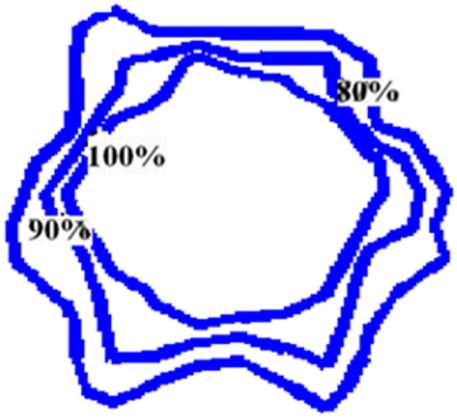


Figure 3. Dose distribution in a slice of pelvic phantom (Up) and isodose curves obtained by gel dosimeter (down).

[Downloaded from ijrr.com on 2026-11-08]

Before irradiation, gels were stored in accelerator room for five hours. Irradiation according to the treatment plan was performed a day after gel preparation using a Varian 2100 linear accelerator and 18 MV photons. The calibration vials were placed in a water tank (40×40×40) and irradiated with 18 MV photons using 20×20 open field and SSD 100 cm. Delivered dose to calibration vials for dose response evaluation was; 1 (2 vials), 2, 4, 6, 7, 8 (2 vials), 9, 10 Gy. A pair of vials was left unirradiated to serve as a control. After irradiation all gels were stored in refrigerator again.

MRI acquisition

Among many feasible methods for gel dosimeter readout and dose mapping, MRI is most popular. During irradiation spin-lattice relaxation rate (R1) and spin-spin relaxation rate (R2) change in gels as a function of absorbed dose, but R2 has a larger sensitivity and dynamic range [4].

MRI imaging was performed 2 days after irradiation using 1.5T scanner (Siemens, symphony) to ensure that polymerization reaction was completed. Gels were placed in MRI room to reach thermal equilibrium and imaging started 5 hours later. The calibration vials were attached to organ-specific inserts and were placed in small water tank for increasing SNR then were positioned at the center of head coil and imaged at the same time. The selected imaging parameters for gels are as follows: the field-of-view (FOV) = 256 mm × 256 mm, slice thickness =5 mm without gap, TR = 5000 ms, echo spacing ΔTE= 22 ms, voxel size = 1mm × 1mm × 5mm, NEX = 2, and the number of echoes = 32.

Image and data processing

After omitting the first echo of the 32-echo train, the R2 values were computed by assuming an exponential decay of the MR signal using an in-house MATLAB code (Mathworks, Inc.). The R2 values of the images converted to dose using calibration equation. Full 3D dose distribution of both measurements and calculations were prepared. On the one hand, because of the different size of organ-specific inserts and calibration vials which cause difference in temperature rise during MRI scanning, and because of potentially higher oxygen contamination in smaller tubes [28], dose scaling in our study is needed to adjust the difference in radiation response of the gels with different sizes. It should be noted that dose scaling was applied on measured dose by comparing the measured dose distribution and corresponding to calculated inside the target volume for relative dosimetry [29].

An important way to evaluate calculated dose distribution, is dose-volume histogram (DVH), and also criteria for the optimization of IMRT treatment plans are often based on DVH constraints [19]. In this study, the unique feature of gel dosimetry (i.e. true 3D dosimetry) was used by calculating dose-volume histogram (DVH) and difference of differential dose-volume histogram (DDDVH) for analyzing. DVH and DDDVH of all defined organs both in calculated and measured data was prepared and compared together. For computing DVH, volumes of interest were defined in both 3D measured and calculated dose distributions and voxels therein were evaluated and then a histogram was mounted.

RESULTS

Calibration data, obtained by the analysis of R2 maps of the calibration screw-top glass vials, are shown in figure 4. After the regression analysis, obtained values are as followings: the slope a=0.838 (± 3.02%) and the offset=5.17 (± 2.28%). Also the coefficient of the determinant R2 and the standard deviation of the R2 value was 0.9973 and approximately 1%, respectively.

As aforementioned, we have limited our results to DVH and difference of differential DVH (DDDVH). Differential dose-volume histogram (DDVH) shows frequency of voxels as a function of specific dose. DDDVH is obtained by subtracting the number of voxels in dose bins for the measured dose from those for the calculated dose [3]. Note that in DDDVH, normalization was performed as dose difference

[Downloaded from ijrr.com on 2026-11-08]

in each bin divided with total number of voxels. If both measured and calculated dose have the same number of voxels with a specific dose range in a bin, it results a value of 0 for that bin. A bar or column height that has value of 0.01, means that there is 1% difference between measured and calculated doses.

Figure 5 shows DVHs and DDDVH for PTV. According to these figures, there was very good agreement between gel-measured and calculated data. In DDDVH figure, dose differences are approximately less than 1%. Nota that 100% dose corresponds to prescribed dose 8Gy. The calculated mean relative dose to the PTV was 100.1±2% (1 SD); while corresponding gel measured value was 101±2.2% (1 SD).

The DVH and DDDVH related to rectum are shown in Figure 6. The DVHs show close agreement between gel-measured and calculated data. Figure (b) shows that measured dose was greater than the calculated dose between 0% (0 Gy) to 4% (0.32 Gy) and was less than the calculated dose between 4% (0.32 Gy) to 10% (0.8 Gy). Beyond 10% (0.8 Gy) dose difference in the DDVH is negligible. The calculated mean relative dose to the rectum was 46±3% (1 SD); while corresponding gel measured value was 44.8±3.3% (1 SD).

Another critical organ is bladder that it's DVHs and DDDVH shown in figure 7. According to DVHs, there are very good agreement between gel-measured and calculated data. Figure 7(b) shows minor deviations that measured dose was greater than the calculated dose between 0% (0 Gy) to 10% (0.8 Gy). Beyond 10% (0.8 Gy) dose difference in the DDVH is negligible.

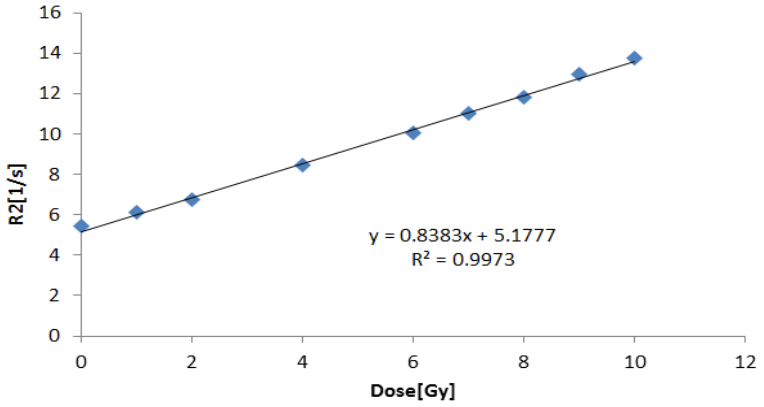


Figure 4.R2 as a function of absorbed dose, the standard deviation of the R2 value was approximately 1%.

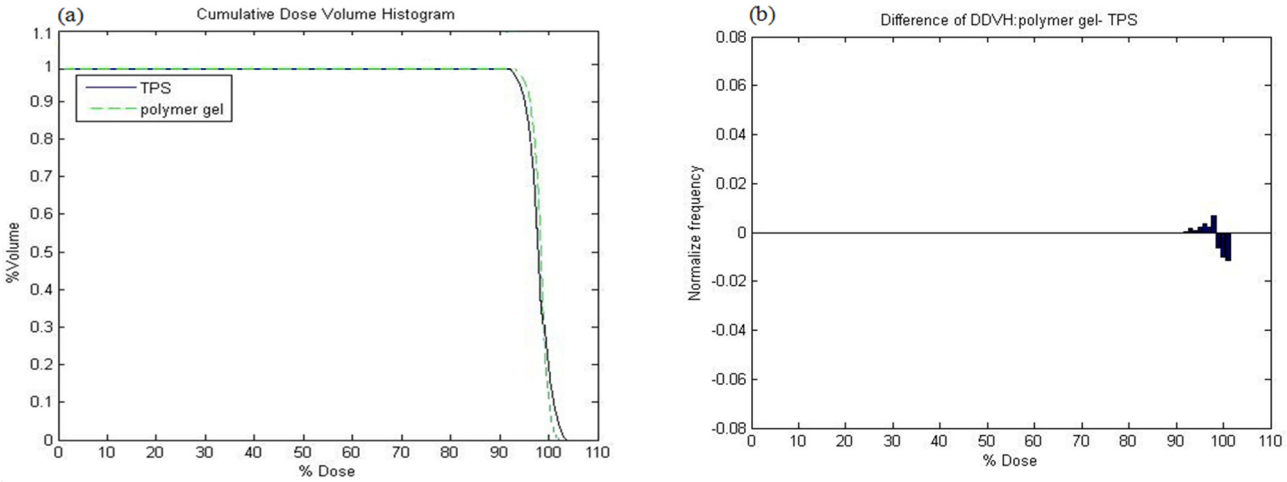


Figure 5. DVH (a) and difference in differential dose-volume histograms (DDDVH) (b) for PTV.

[Downloaded from ijrr.com on 2026-11-08]

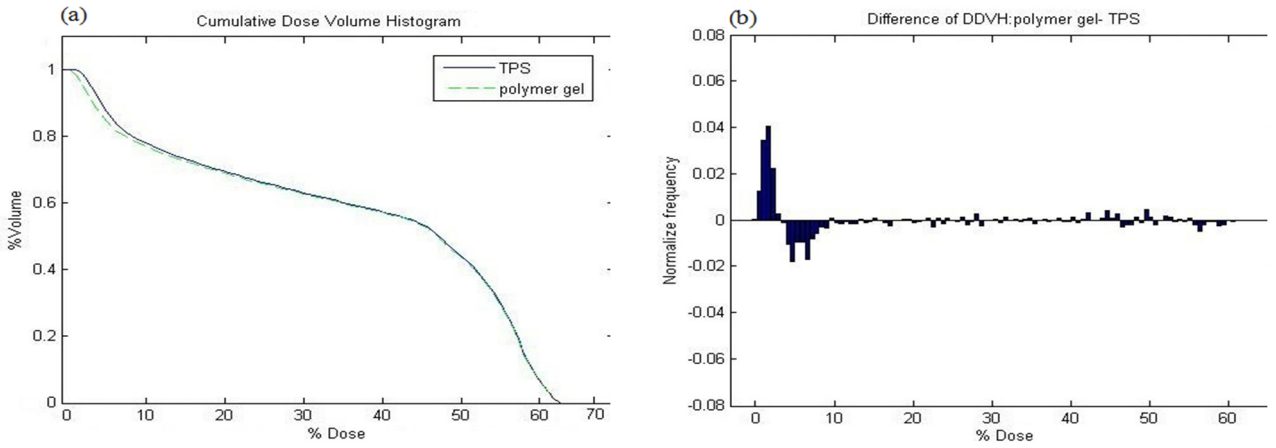


Figure 6. DVH (a) and difference in differential dose-volume histograms (DDDVH) (b) for rectum.

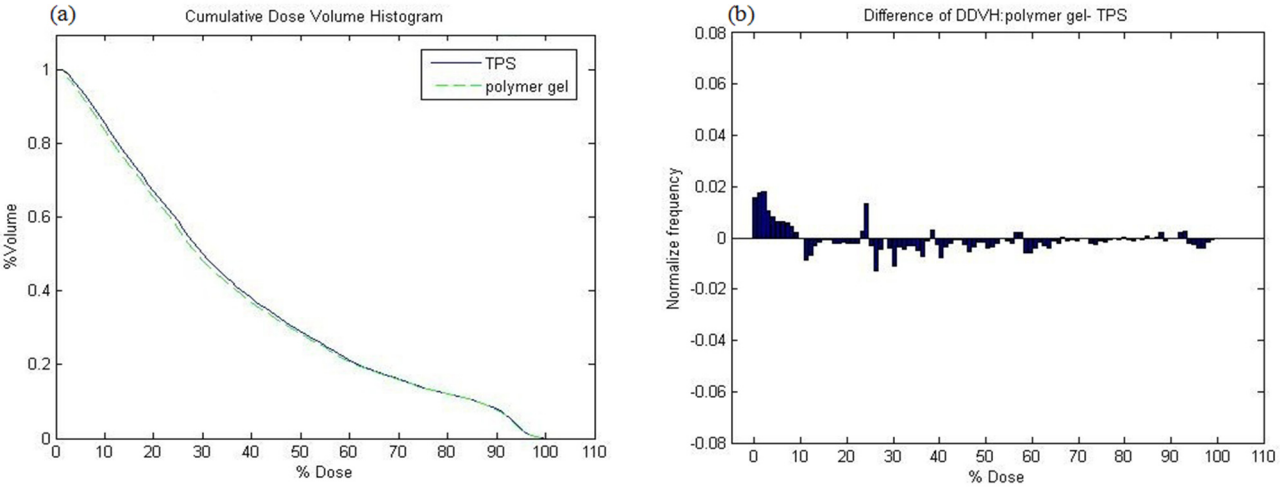


Figure 7.DVH (a) and difference in differential dose-volume histograms (DDDVH) (b) for bladder.

DISCUSSION

Comparison between calculated dose distribution and corresponding to measurement can be carried out by many ways. For current study, we used DVH and DDDVH for comparison. According to results for PTV, there was high degree of agreement between measured and calculated data for PTV. Also obtained results for organ at risks show overall good agreement between measured and calculated data.

As mentioned in introduction, application of gel dosimetry for treatment plan verification in MLC-based IMRT has been investigated by many researchers in homogeneous phantom. Gustavsson et *al.* [19] investigated the feasibility of using new type gel for IMRT verification. They filled a cylindrical glass flask with gel as phantom, a kidney-shaped target was defined and planning was based on sliding window technique. According to their results, there was good agreement between measured end calculated dose distribution, discrepancies were found in hot spots the upper and lower parts of PTV and this was attributed to sub optimal scatter kernels used in TPS.

Sandilos *et al.* [24] for validating TPS, captured dose distribution by gel dosimetry for a prostate MLC-based treatment plan configuration and their results showed gel-measured dose distributions were adequately matched with corresponding TPS calculations.

Vergote *et al.* [25] used thorax phantom for validating TPS in presence of air inhomogeneity and their results showed an underdosage of the

[Downloaded from ijrr.com on 2026-11-08]

PTV and concluded that polymer gel dosimetry is a valuable technique to verify dose calculation algorithms for IMRT in heterogeneous configurations.

Farajollahi [26] assessed the accuracy of the predicted dose distribution in prostate compensator-based IMRT plan using both gel and film. A cylindrical homogeneous phantom was used. The 90% isodose line from the film measurement was superimposed on the gel results together with the calculated 90% isodose line. There was reasonable agreement between two methods, but both showed similar discrepancies in some regions compared with the calculations. Possible reasons for these discrepancies were attributed to slight error in the settings of the beams or the positioning of the compensator, or more obviously in the algorithm used in the calculation.

Haas [27] investigated to verify an compensator-based IMRT plan in head and neck phantom using film and gel dosimetry. There was good agreement between the dose distribution obtained with film and gel dosimetry, some discrepancies were observed between calculated and measured dose distribution. These discrepancies were attributed to compensator manufacturing process; this was because of limitation of the milling machine used to manufacture the compensators in producing beam profile accurately.

Comparison between our results and others confirms the applicability of gel dosimetry for 3D dose verification in IMRT and shows predicted dose distribution by TiGRT in the presence of bone-equivalent inhomogeneity has acceptable accuracy.

It should be noted that the use of glass vials reduce the uncertainty of R2 calculation close to vial edges and the use of smaller vials reduce the cost relative to using larger vials.

CONCLSIONS

An experimental procedure based on the MRI-polymer gel dosimetry method was used to verify a compensator-based IMRT plan in inhomogeneous phantom. According to the results, it can be concluded that used treatment plan configuration in the presence of inhomogeneity has clinically acceptable accuracy and gel dosimetry is a useful tool for measuring DVH to compare it with treatment planning system results, hence it can be used for compensator-based IMRT treatment verification and quality assurance.

REFERENCES

1. Papanikolaou N, Battista J, Boyer A, Kappas C, Klein E, Mackie T, Sharpe M, Van Dyk J (2004) Tissue inhomogeneity corrections for megavoltage photon beams. *AAPM Task Group,* ***65:*** *1-142*
2. Ezzell GA, Galvin JM, Low D, Palta JR, Rosen I, Sharpe MB, Xia P, Xiao Y, Xing L, Cedric XY (2003) Guidance document on delivery, treatment planning, and clinical implementation of IMRT: Report of the IMRT subcommittee of the AAPM radiation therapy committee. *Medical Physics,* ***30:****2089-115.*
3. Watanabe Y and Gopishankar N (2010) Three-dimensional dosimetry of TomoTherapy by MRI-based polymer gel technique. *Journal of Applied Clinical Medical Physics,* ***12:*** *(1) 3273.*
4. Baldock C, De Deene Y, Doran S, Ibbott G, Jirasek A, Lepage M, McAuley KB, Oldham M, Schreiner LJ (2010) Polymer gel dosimetry. *Physics in Medicine and Biology, [Review]. Mar 7;55* ***(5)****:R1-63.*
5. Deene YD (2004) Essential characteristics of polymer gel dosimeters. *J Phys: Conf Ser,* ***3:*** *34-57.*
6. Fong PM, Keil DC, Does MD, Gore JC (2001) Polymer gels for magnetic resonance imaging of radiation dose distributions at normal room atmosphere. *Physics in Medicine and Biology,* ***46:*** *3105.*
7. Brahme A (1988) Optimization of stationary and moving beam radiation therapy techniques. *Radiotherapy and Oncology,* ***12(2):****129-40.*
8. Chang S (2006) Compensator-intensity-modulated Radiotherapy—A traditional tool for modern application. *US Oncological Disease,* ***115:*** *1-4.*
9. Chang SX, Cullip TJ, Deschesne KM (2000) Intensity modulation delivery techniques: "Step & Shoot" MLC auto-sequence versus the use of a modulator. *Medical Physics,* ***1(2):*** *80-85.*
10. Chang SX, Cullip TJ, Deschesne KM, Miller EP, Rosenman JG (2004) Compensators: an alternative IMRT delivery technique. *Journal of Applied Clinical Medical Physics,* ***5(3):*** *15-36.*
11. Chang SX, Deschesne KM, Cullip TJ, Parker SA, Earnhart J (1999) A comparison of different intensity

[Downloaded from ijrr.com on 2026-11-08]

modulation treatment techniques for tangential breast irradiation. *International Journal of Radiation Oncology Biology Physics,* ***45(5):****1305-14.*

12. Srivastava RP and De Wagter C (2007) The value of EDR2 film dosimetry in compensator-based intensity modulated radiation therapy. *Physics in medicine and biology,* ***52:****N449.*
13. Wendt TG, Abbasi-Senger N, Salz H, Pinquart I, Koscielny S, Przetak SM, Wiezorek T (2006) 3D-conformal-intensity modulated radiotherapy with compensators for head and neck cancer: clinical results of normal tissue sparing. *Radiation Oncology,* ***1(1):*** *1-18.*
14. Xu T, Shikhaliev PM, Al-Ghazi M, Molloi S (2002) Reshapable physical modulator for intensity modulated radiation therapy. *Medical physics,* ***29:*** *2222-2229.*
15. Jiang SB and Ayyangar KM (1998) On compensator design for photon beam intensity-modulated conformal therapy. *Medical physics,* ***25:*** *668-75.*
16. Vaezzadeh S, Allahverdi M, Nedaie HA, Ay M, Shirazi A, Yarahmadi M (2013) EBT GAFCHROMIC™ film dosimetry in compensator-based intensity modulated radiation therapy. *Medical Dosimetry, 38(2): 176-83.*
17. Crescenti RA, Scheib SG, Schneider U, Gianolini S (2007) Introducing gel dosimetry in a clinical environment: customization of polymer gel composition and magnetic resonance imaging parameters used for 3D dose verifications in radiosurgery and intensity modulated radiotherapy. *Medical physics,* ***34:*** *1286-97.*
18. Gopishankar N, Vivekanandhan S, Rath G, Laviraj M, Senthilkumaran S, Kale S, Thulkar S, Bisht R, Subramani V (2013) Indigenously developed multipurpose acrylic head phantom for verification of IMRT using film and gel dosimetry. *Journal of Applied Clinical Medical Physics,* ***14 (2):*** *62-76.*
19. Gustavsson H, Karlsson A, Bäck SÅJ, Olsson LE, Haraldsson P, Engström P, Nyström H (2003) MAGIC-type polymer gel for three-dimensional dosimetry: Intensity-modulated radiation therapy verification. Medical physics, ***30:*** *1264-71.*
20. Karlsson A, Smulders B, Gustavsson H, Bäck SÅJ, editors. (2004) IMRT prostate dosimetry using a normoxic polymer gel and MRI. *J Phys; Conf. Ser,* ***3:*** *284-287.*
21. Low DA, Dempsey JF, Venkatesan R, Mutic S, Markman J, Haacke EM, Purdy JA (1999) Evaluation of polymer gels and MRI as a 3-D dosimeter for intensity-modulated radiation therapy. *Medical physics,* ***26:*** *1542-51.*
22. Oldham M, Gluckman G, Kim L, editors (2004) 3D verification of a prostate IMRT treatment by polymer gel-dosimetry and optical-CT scanning: *J Phys; Conf Ser,* ***3:*** *293-296.*
23. Pavoni J, Pike T, Snow J, DeWerd L, Baffa O (2012) Tomotherapy dose distribution verification using MAGIC-f polymer gel dosimetry. *Medical Physics,* ***39:*** *2877-84.*
24. Sandilos P, Angelopoulos A, Baras P, Dardoufas K, Karaiskos P, Kipouros P, Kozicki M, Rosiak JM, Sakelliou L, Seimenis I (2004) Dose verification in clinical IMRT prostate incidents. *International Journal of Radiation Oncology* Biology* Physics,* ***59(5):****1540-7.*
25. Vergote K, De Deene Y, Claus F, De Gersem W, Van Duyse B, Paelinck L, Achten E, De Neve W, De Wagter C (2003) Application of monomer/polymer gel dosimetry to study the effects of tissue inhomogeneities on intensity-modulated radiation therapy (IMRT) dose distributions. *Radiotherapy and Oncology,* ***67(1):****119-28.*
26. Farajollahi AR (1998) An investigation into the applications of polymer gel dosimetry in radiotherapy. *Medical Physics,* ***26****: 493*
27. Haas O (2003) An intelligent oncology workstation for the 21st century. *NOWOTWORY,* ***53(4):*** *389-97.*
28. MacDougall N, Miquel M, Keevil S (2008) Effects of phantom volume and shape on the accuracy of MRI BANG gel dosimetry using BANG3TM. *British Journal of Radiology,* ***81(961):****46-50.*
29. Watanabe Y (2005) Variable transformation of calibration equations for radiation dosimetry. *Physics in Medicine and Biology,* ***50(6):*** *1221-34.*

[Downloaded from ijrr.com on 2026-11-08]